INTEGRATING 4D SEISMIC INTERPRETATION AND WATER SATURATION ESTIMATION IN THE WELL REPOSITION: APPLICATIONS IN MARLIM FIELD, CAMPOS BASIN, BRAZIL

Caio Jean Matto Grosso da Silva [1], Pedro Benac [2], Erick Botelho[1],

Hilario Mucelini Giro[1], Rosenberg Lima[1], Paula Freitas Santos[1], Matheus de Almeida Garcia[1],

Thiago Camanho[1], and Carlos Alexandre Pedrosa[1]

[1]Petrobras, Macaé, RJ, Brazil
[2]Petrobras, Rio de Janeiro, RJ, Brazil

*Corresponding author email: cjmgs@petrobras.com.br

ABSTRACT. In 2022, Petrobras launched its first revitalization project: the Marlim and Voador Revitalization Project (REVIT). This initiative aims to extend productive life of the Marlim Field, situated on Campos Basin, Brazil, which has been in operation for the last three decades. To achieve this goal, the project scope entails replacing eight existing platforms in the fields with two new platforms. The operation will involve managing a total of 75 wells of which, 14 will be new producer wells situated in the Marlim post-salt reservoir composed of turbidite lobes. To assist project implementation, 4D seismic data has been highlighted as an essential tool for identify unswept areas and delineate new well locations. However, reviewing the original well locations from 4D seismic requires a team analysis that integrates it with information from several knowledge areas such as geophysics, geology, and engineering. In a mature field, like Marlim, information on wells construction and submarine facilities is also necessary. These analyses take time impacting the project schedule. To mitigate this impact, it was proposed a calculation of water saturation from 4D seismic inversion results to support the 4D interpretation and speed up the necessary analysis. This estimated attribute has simplified the search for new areas to location optimization.

Keywords: Gassmann's equation; time-lapse seismic; quantitative interpretation; reservoir management.

INTRODUCTION

Time-lapse seismic, also known as 4D seismic, is a very important and useful technology to management reservoir. This method compares repeated 3D seismic surveys over a same area to make images that illustrate, for example, fluid flow and pressure changes in the lifetime of a reservoir. Ribeiro et al. (2005) evaluates the

feasibility of using this technology in Marlim and since 2005 this technology has been applied in Marlim reservoir. The firsts work in 4D seismic monitoring are from North Sea (Landrø, et al., 1999; Boyd-Gorst et al., 2001). Since then, 4D has been applied to several kind reservoir (Burkhart et al., 2000; Johann et al., 2006; Webb et al., 2020) even for stiffer Albian carbonates reservoir (Grochau et al., 2014) or Brazilian pre-salt carbonates (Cruz et al., 2021). The Marlim sandstones of Marlim Field is a post-salt reservoir located on Campos Basin. It spans an area around 150 km² and is composed by turbidites of excellent permeability and porosity features (Oliveira et al., 2007). The oil production history of this reservoir started in 1991 and by 1997 the base seismic data for future 4Ds surveys was acquired. To maintain the mass balance between produced and injected liquids and ensure a stable pressure level, water injection into the reservoir was initiated in 1994. Given this, along with a good hydraulic connectivity observed in the reservoir, high 4D pressure effects are not anticipated. In simpler terms, the primary factor contributing to 4D anomalies is expected to be related to fluid substitution.

In addition to the turbidite reservoir, Marlim and Voador fields also contain a pre-salt reservoir. Discovery in 2010, this reservoir rock features a laminated structure with a variety of permeable and porous characteristics, exhibiting an average porosity and permeability of 7% and 90 mD, respectively. Notably, certain layers display significantly higher permeability and porosity than the average, creating zones with substantial hydraulic connectivity. However, the reservoir' stiffness, coupled with a modest production during that period between time-lapse seismic monitoring, has hindered the observation of 4D anomalies associated with production from this reservoir.

In 2005 and 2010, two new 4D seismic monitors were acquired and provided information to several 4D applications on Marlim reservoir, as updating the geological model contributing to the improvement in the history match (Oliveira et al., 2007) or manage the reservoir (Sansonowski et al, 2007). The most recent 4D seismic acquisition on Marlim was finished in April 2022. Therefore, there are three different time intervals (1997-2005, 2005-2010 and 2010-2022) for 4D analysis. A time-lapse inversion, also known as 4D inversion, is a powerful tool that assists geophysicists in seismic interpretation by providing several benefits, such as quantitative estimates of impedance changes that are useful for calibrating and understanding the rock physics models (Johnston, 2013 and Villaudy et al., 2013). Sarkar et al. (2003) and Rosa et al. (2020) have analyzed various 4D inversion processes. Generally, these processes can be classified into two main groups. The first group is commonly referred to as sequential independent 3D inversion, where each seismic base vintage is inverted separately, followed by the other 3D seismic surveys. The second group is known as joint 4D inversion, where multiple 4D seismic vintages are inverted simultaneously (Lafet et al., 2008; Buland and El Ouair, 2006). To initiate the 4D seismic interpretation, it was performed a sequential independent 3D inversion for each time interval,

resulting in three 4D Acoustic Impedance variation (Delta Impedance) volumes. This attribute helped us to distinguish between hardening and softening 4D signals. To speed up the analysis, initially, we interpreted the 4D impedance data using the whole-time interval that is the differences observed between 2022 and 1997. Once identified unswept areas in the reservoir at this time interval (2022-1997), we analyzed the other intervals to evaluate if any 4D effect could be underrated due to potential destructive seismic interference.

As mentioned, despite the value of this single Delta Impedance volume (2022-1997), it is important to analyze each separated vintage data. However, looking for new potential areas become easier, once the first step can be evaluated from a single data instead of three.

This analysis had a significant favorable impact on the Marlim and Voador Revitalization Project (REVIT) well drilling schedule. Nevertheless, we faced the challenge of evaluating 14 new well locations. The task of assessing potential area was driven by a multidisciplinary team of professional, with some of them were less familiar with the concept of elastic property information, derived from 4D seismic.

To enhance communication across different disciplines, transform P-Impedance changes into water saturation changes can be very helpful. However, due to the ambiguity of pressure and saturation effects on elastic parameters, quantifying them is not a simple task. Nevertheless, the literature provides several methods for conducting this quantitative analysis. One approach to discriminate and quantify changes in saturation and pressure is through amplitude versus offset (AVO) analysis

(Landrø, 2001; Landrø et al., 2003; Bhakta and Landrø, 2014). Another methodology involves a good understanding of rock physics models, from we can establish relationships between elastic properties and pressure and saturation changes (Lumley et al., 2003; Ribeiro and MacBeth, 2004; Damasceno, 2020; Damasceno et al., 2021). By using 4D seismic attributes as constraints is even possible to establish relationships independently of the rock physics model to obtain changes in saturation and pressure (Floricich et al., 2005; MacBeth et al., 2006).

Based on a simple rock physics model, we proposed an approach aimed to estimate water saturation from 4D seismic inversion results using Gassmann's equation. This technique served as a bridge to fill the gap and facilitate understanding among the team members, ultimately fostering more effective decision-making.

The results achieved provided enough information to allow the needed adjustments of the well locations with good matching of project's schedule. Moreover, the results exhibit a good correlation between production data and well log data, reinforcing their reliability and relevance.

METHODOLOGY

A fundamental information to the 4D seismic water saturation estimation process, proposed in this work, is the knowledge of the P-Impedance variation in the whole reservoir. The way to obtain this information is performing a 4D seismic inversion. In the literature, there are several seismic inversion methods available, for instance sparse spike, model based and

recursive inversion (Veeken and Da Silva, 2004). For this work, we use a sparse spike inversion method. It is important to emphasize that the reliability of water saturation estimation from 4D seismic rely on the quality of the results of the 4D seismic inversion.

To develop this work was needed a petroelastic model that allow us to estimate the impedance for different fluid saturation conditions. Smith et al. (2003) stated that one of the most commonly theoretical approach for fluid substitution can be obtained by Gassmann's equation. In fact, Gassmann (1951) developed a petroelastic model, one of the most important tools for exploration and reservoir geophysics, that describes the elastic behavior of saturated rock. According to this model, we can calculate a saturated rock bulk modulus, K_{Sat}, necessary to estimate the impedance, presented in Eq. (1):

$$\frac{K_{Sat}}{K_M - K_{Sat}} = \frac{K_{Dry}}{K_M - K_{Dry}} + \frac{K_F}{(K_M - K_F)\phi}, \quad (1)$$

where, K_{Sat}, K_{Dry}, K_F and K_M are the bulk moduli of saturated rock, dry rock, fluid, and mineral, respectively, and ϕ is the rock porosity. To elaborate the equation, Gassmann (1951) made some assumptions as, for instance: a rock composed of homogeneous mineral and saturated by a homogeneous fluid. Grochau and Gurevich (2008) conducted tests in some of these assumptions and validated it to time-lapse applications. Additionally, Rasolofosaon and Zinszner (2007) have demonstrated that despite the fact of Gassmann's theory be a quasi-static theory in principle, it can explain experimental results even beyond its domain of applicability.

Anyway, it is needed to simplify the rock and fluid mixture to be able to use Gassmann's equation. Avseth et al. (2005) quotes as useful and adequate use as the value of the homogeneous mineral an average between the maximum and minimum possible limits calculated for it. In our work, the limits were obtained by Voight and Reuss average (Avseth et al., 2005). Voight average and Reuss average are presented in Eq. (2) and Eq. (3).

$$M_V = \sum_{i=1}^{N} f_i M_i, \quad (2)$$

$$\frac{1}{M_R} = \sum_{i=1}^{N} \frac{f_i}{M_i}, \quad (3)$$

where, f_i and M_i are the volume fraction and elastic modulus of the i constituent, respectively.

The fluid case presents a relatively simpler scenario when compared to mineral, because the stress is equally distributed between the phases, then Reuss average correspond to the mixture modulus. To estimate the fluid moduli and density of each fluid (gas, oil and water), we used the Batzle and Wang (1992) equations to evaluate them, starting from some reservoir properties as: temperature, pressure, gas-oil ratio, API, salinity and gas specific gravity.

Therefore, combining all these information, it is possible to use Gassmann's equation and obtain a saturated rock bulk modulus with a chosen mixture of fluids.

Figure 1 shows the bulk modulus of a saturated rock at various saturation levels considering a two-phase mixture of oil and water. This distribution was derived using the average

reservoir properties presented in Table 1. Fluid elastic properties used to build the curve were calculated using the petrophysical properties presented in Table 2 and the methodology developed by Batzle and Wang (1992).
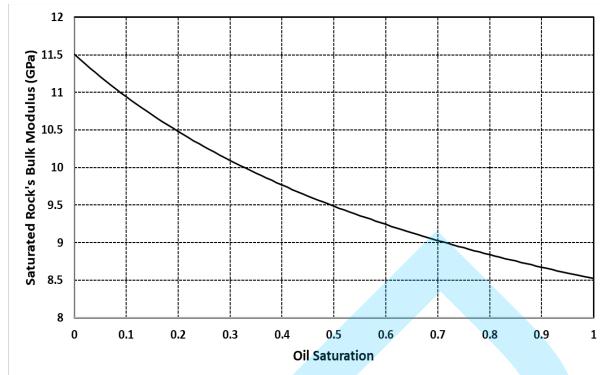
Figure 1 – *Saturated rock's bulk modulus as a function of fluid saturation.*

Table 1 – *Average (μ) and standard deviation (δ) of dry rock bulk modulus (K_{Dry}), shear modulus (G), porosity ($\emptyset$) and mineral bulk modulus (K_M).*

|	K_{Dry}	G	ϕ	K_M
μ	5.8 GPa	3.7 GPa	28%	33.2 GPa
δ	1.5 GPa	0.5 GPa	4%	3 GPa

Table 2 – *Environmental conditions and fluid properties. From left to right: temperature, pore pressure, salinity, API, gas-oil ratio and gas specific gravity.*

| T	P_p	Sal	API	GOR	S. G.
70 °C	26.5 MPa	56.000 ppm	20°	78	0.635

To estimate impedance is necessary first obtain the density of the saturated rock that can be obtained from a mass balance equation for density; and the shear modulus is not sensitive to the fluid, thus it becomes feasible to derive, from the saturated rock bulk modulus, the P-Velocity and subsequently the P-Impedance as a function of fluid saturation as expressed in Eq (4):

$$V_P = \sqrt{\frac{K + \frac{4}{3}\mu}{\rho}} \implies I_p = V_p\rho \qquad (4)$$

Figure 2 shows the P-Impedance behavior as a function of water and oil mixture fluid level (oil saturation, S_{Oil}, and water saturation, S_w). If we designate a specific point in x-axis, such as 15%, to represent the initial water saturation (corresponding to 85% oil saturation), then it is easy to calculate the P-Impedance variation (ΔP_I) in response to fluctuation in water saturation (ΔS_w) from that initial point, as showed in Figure 2. It is important to highlight that as we consider a two-phase fluid mixture, then we can easily use ΔS_w or ΔS_{Oil} (oil saturation variation) in our calculations. Performing this calculation for each point starting from the initial one, it is possible to obtain a curve of P-Impedance variation as a function of water saturation variation, as shown in Figure 3.
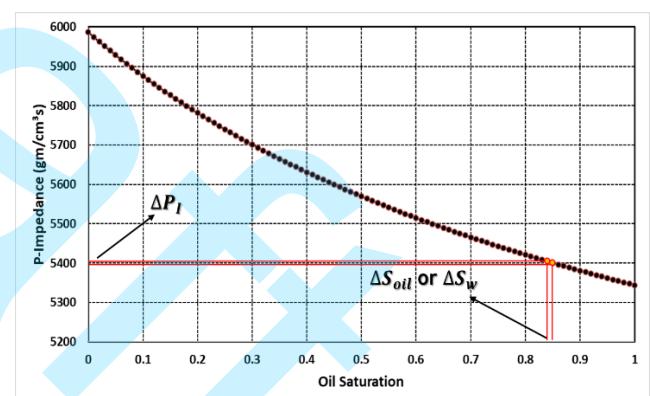

Figure 2 – *P-Impedance as a function of fluid saturation. In the figure is also presented the P-Impedance variation (ΔP_I) for a single water saturation variation (ΔS_w) or oil saturation variation (ΔS_{Oil}).*
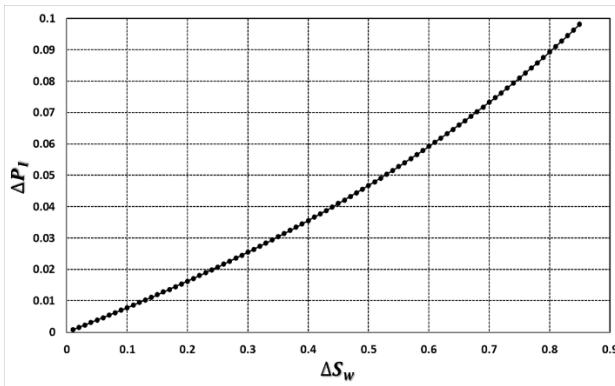
Figure 3 – *P-Impedance variation* (ΔP_I) *as a function of water saturation variation* (ΔS_w).

By swapping the x-axis with the y-axis, then it is possible to derive a distribution of variation in water saturation as a function of changes in P-Impedance, as presented in Figure 4. Subsequently, fine-tuning a regression model to the data points distribution, we can derive an inverse function for converting P-Impedance variations into water saturation variations. Given that a 4D seismic inversion enable us to calculate impedance variation in the whole reservoir, therefore, we can apply the regression model shown in Figure 4 to derive an estimate of 4D water saturation distribution.
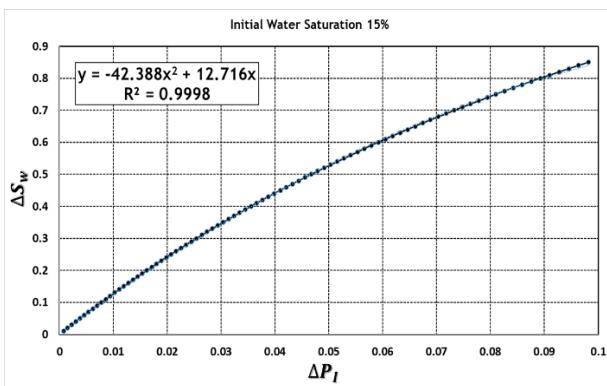
Figure 4 – *Water saturation variation* (ΔS_w) *as a function of P-Impedance variation* (ΔP_I).

The function obtained for the Marlim reservoir case, and showed in Figure 4, is given by:

$$y = -42.388x^2 + 12.716x \qquad (5)$$

Assumptions

The curve fitted to the data points, shown in Eq. (5), represents an inversion function based on the most basic petroelastical model that could be built from the average properties. Consequently, the accuracy of the calculated water saturation values depends on the adequacy of this simple model in representing the reservoir. Essentially, applying this inversion function to estimate 4D volumetric data involves making certain assumptions, as the reservoir has features that vary spatially.

In the following, we will discuss four assumptions to analyze if although the estimated values may not be perfectly accurate, they can still provide useful information and serve as a valuable tool for identify unswept areas.

1. Two-phase Fluids Condition

In the way the problem was presented for the specific case of the Marlim turbidite reservoir, it is observed that the estimate is valid only for a fluid mixture composed of oil and water only. Therefore, there is an implicit assumption that can be appropriately parameterized for different cases.

2. Initial Water Saturation Level

As shown in Figure 4, the curve exhibits a non-linear pattern, indicating that the same impedance variation can result in different estimated saturation values, this depending on the initial saturation conditions. Therefore, it is important to have an estimate of the initial saturation level to increase confidence in the outcome of the curve. While saturations may vary across different regions, the proximity of

the initial value used to the actual saturation will determine how closely the results align with the correct answer. Based on production data and in the flow model we can estimate the oil recovered fraction and indicate how much is the mean water saturation level in the reservoir at any time. Then, we assumed saturation levels for each vintage near that observed in our data and model. Therefore, we assumed the saturation in 1997 and 2005 was 15% and in 2010 was 35%. However, they are far from represent the heterogeneous in a mature field as Marlim, but we believe these choices reduce the impact of the current assumption.

3. Average Petrophysical Properties

The third assumption assumes that there is no variation in the average values of the petrophysical properties used to construct the curve shown in Figure 4, as the data points were calculated using the average properties of the reservoir. Although the Marlim reservoir is considered relatively homogeneous, two scenarios were developed to evaluate the uncertainties introduced when this assumption is not met.

The curve in Figure 4 served as the base scenario and two additional scenarios were created based on the average values and standard deviation of the properties (Table 1). To do this, we added or subtracted the standard deviation values to the average values in order to generate two opposite rock physics models. Although using just one standard deviation to construct new scenarios does not encompass all possible uncertainty, we justify its use because the standard deviation was obtained

using well log data, which has a higher frequency content than seismic data. Therefore, the distribution based on well log data will be more spread out than seismic data, resulting in larger standard deviations. Figure 5 shows the results of this analysis.
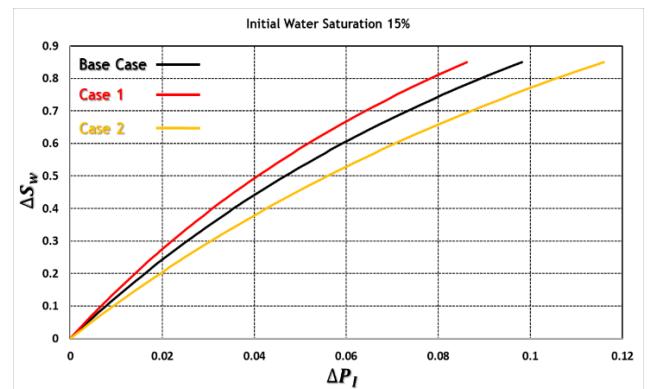
Figure 5 – *Impact of change in properties in the function to estimate saturation.*

As expected, there is a deviation in saturation estimates for the same impedance variation, and this deviation becomes more noticeable with increasing 4D signal response. However, it is observed that the dispersion is not excessively wide. For example, in the scenario shown in Figure 5, with a Delta P-Impedance of 6% the corresponding water saturation increase in the base scenario is 59%. In contrast, in the optimistic or pessimistic scenarios, the water saturation increase would be 55% or 65%, respectively. Despite the range of uncertainty, this still provides valuable information regarding the magnitude order of water saturation variation.

4. Negligible Effect of Pressure

A critical assumption in this approach is that the observed anomalies in the 4D seismic data are exclusively attributed to saturation effects. It is known that pressure change can also influence

impedance. Therefore, the application of the function will only be valid in areas where there is no change in pressure.

In the Marlim reservoir, the pressure was well controlled through the water injection process, and the reservoir has good hydraulic communication characteristics. As a result, only minor pressure variations have been observed. For example, based on the flow model the major difference in pressure observed in the period between 2022 and 2010, should be around 2 MPa. Although these variations can have some influence on the water saturation estimates, the observed results indicate that the interference remains relatively minimal.

RESULTS

As mentioned, there are three different time intervals (2005-1997, 2010-2005 and 2022-2010) of 4D seismic data. While the individual analysis of these intervals is important, analyze the complete interval (2022-1997) could reveal a more complex reservoir than previously thought, as showed by Figure 6. The figure shows, in a 3D view, geobodies extracted from the 4D P-Impedance data, spanning the period between 2022 and 1997. To extract geobodies, we defined a window between the limits of the reservoir and discard very low and negative values of P-Impedance variations (ΔP_I). For the whole seismic data interval (2022-1997), based on our production data, we do not expect softening 4D anomalies. In fact, we do not observe 4D negative anomalies. When negative values are observed in the 4D seismic data, they are very sparse and have low magnitude representing 4D noise or, in some cases, wavelet side lobes that could not be removed in the inversion process. The arrows in the figure indicate the preferential paths of fluid movement that were inferred based on our conceptual depositional model. These preferential paths are believed to correspond to depositional lobes that could control the fluid flow dynamics within the reservoir, revealing anisotropy control.

A gamma ray log of a well within the reservoir is showed in Figure 6. The well position is highlighted in the figure by the red dot.
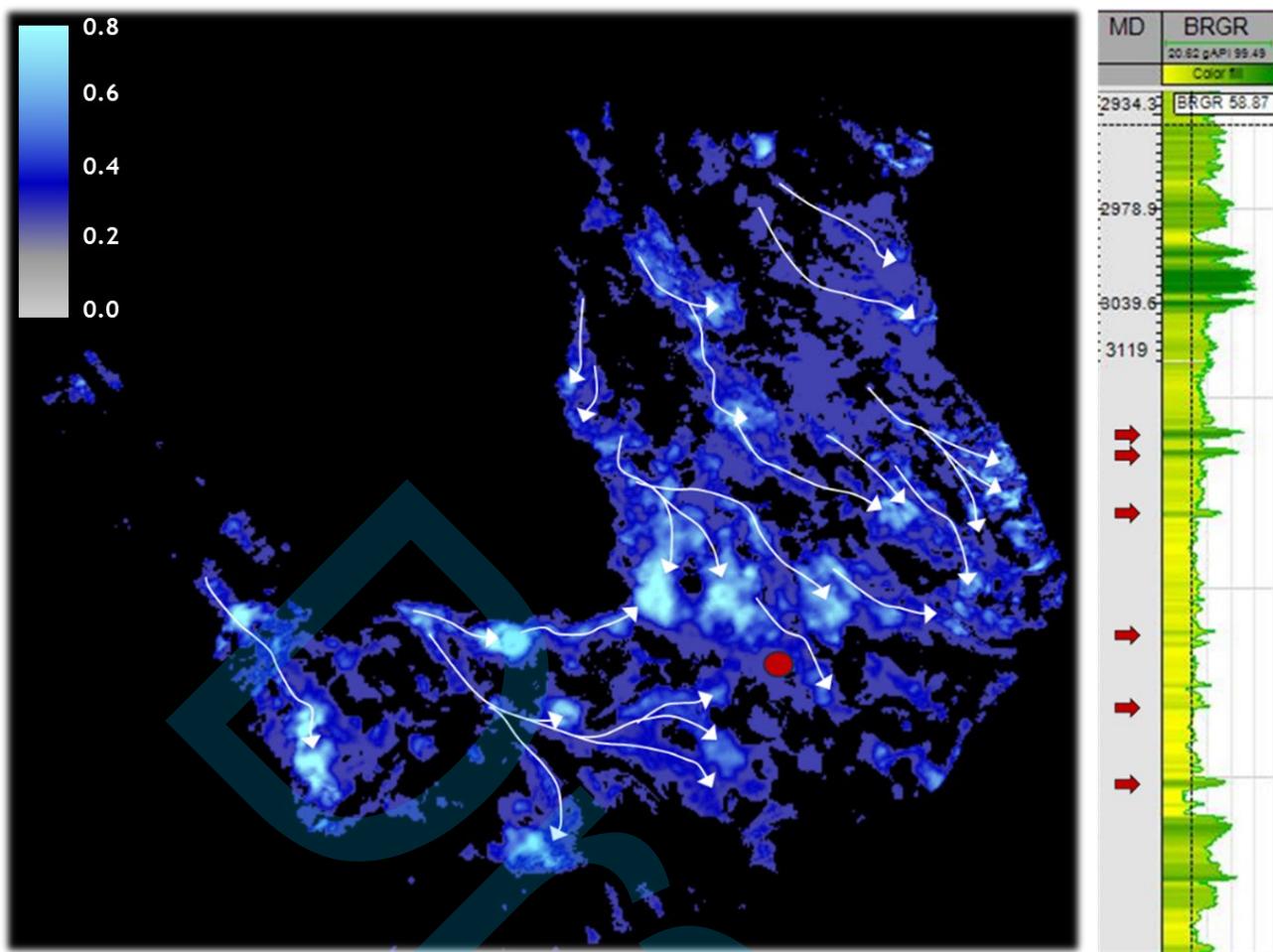
Figure 6 – 3D view of *geobodies extracted from 4D P-Impedance data between 2022 and 1997. Gamma ray (BRGR) log of a well located in the red circle. The red arrows in the figure indicate the presence of thin layers of the shale.*

These preferential paths represent an information that has proven to be very useful as it provides a better understanding of the reservoir. It reveals information that is difficult to observe in conventional 3D seismic data, especially when anisotropy is influenced by thin layers of shale. A gamma ray log, extracted from the well located in the red dot in the Figure 8, illustrate, with red arrows, the position of these thin layers capable of control the flow fluid in the reservoir. While these thin layers may not be directly visible in 4D seismic data, their existence can be inferred by observing the behavior of water path within the reservoir. This inference can lead to a better understand of the dynamics water flow within the reservoir, which can be utilized in the updating process of our reservoir flow models.

Figure 7-A shows a 4D mean P-Impedance map for the period between 2022 and 1997. As already explained, also for this figure we only consider the positive values once we did not observe consistent softening anomalies, using the methodology previously described the variation in water saturation was estimated from the 4D seismic data. The water saturation was estimated for each voxel from the 4D seismic volume. An average map of water saturation for the period between 1997 and 2022, was then calculated, as shown in Figure 7-B. A quick comparison between Figures 7-A and 7-B allows us to conclude that the calculation only

involved a scale conversion between the two properties without losing or creating any information.

Figure 7-B shows the variation in water saturation observed during the time interval from 1997 to 2022. Since seismic data prior to 1997 is not available, it is not possible to accurately assess the change in water saturation before that time. To gain a better understand of the water saturation state, the water saturation determined by the flow model in 1997 was incorporated into the 4D water saturation variation. This incorporation was done because the production and water injection between 1991 and 1997 was relatively modest.
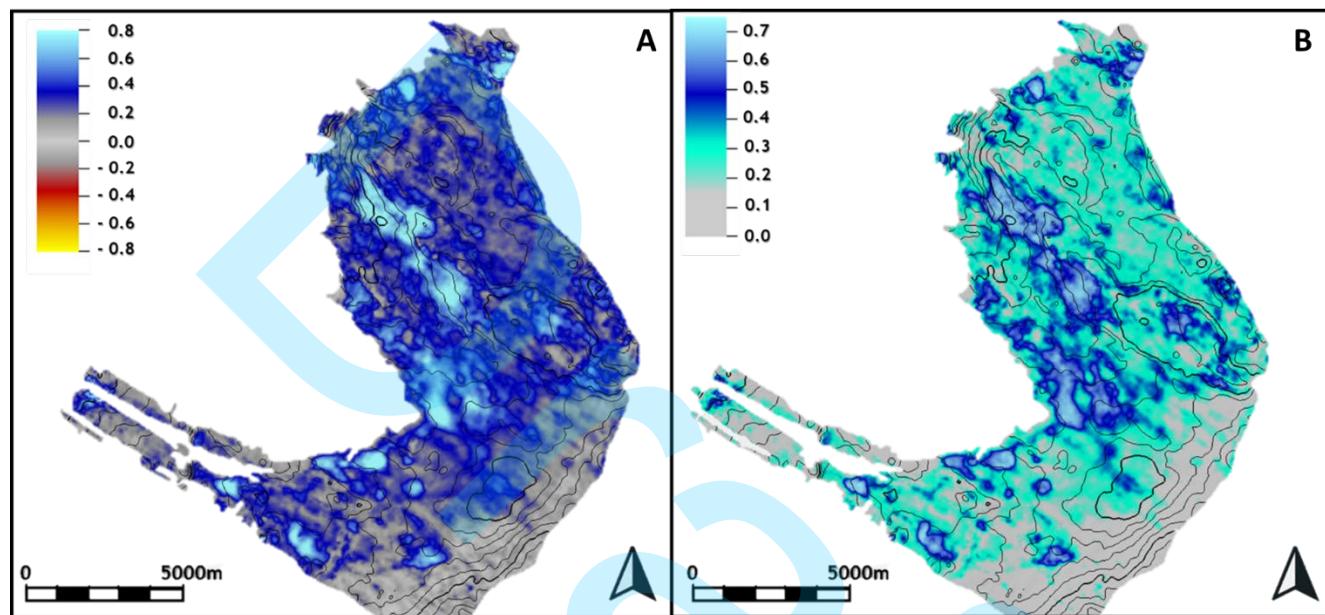
Figure 7 – *4D attributes maps. (A) mean P-Impedance variation observed between 2022 and 1997; (B) mean water saturation variation estimated from 4D seismic between 2022 and 1997.*

Once the water saturation state is calculated from 4D seismic data, it is possible to use it to estimate an oil saturation or even create a residual oil map when combined with thickness data and porosity, as shown in Figure 8. This combined approach makes the map a more efficient tool for identifying new opportunities compared to a traditional 4D map. Unlike a binary analysis typically used in a 4D map (with or without 4D anomaly), the residual oil map incorporates 4D information and combine it with other reservoir properties allowing for a more comprehensive analysis. Ultimately, the residual oil thickness map can help expedite the search for well target adjustments. In the map we can also see the adjustment that were required for the 14 planned producer wells in the REVIT.
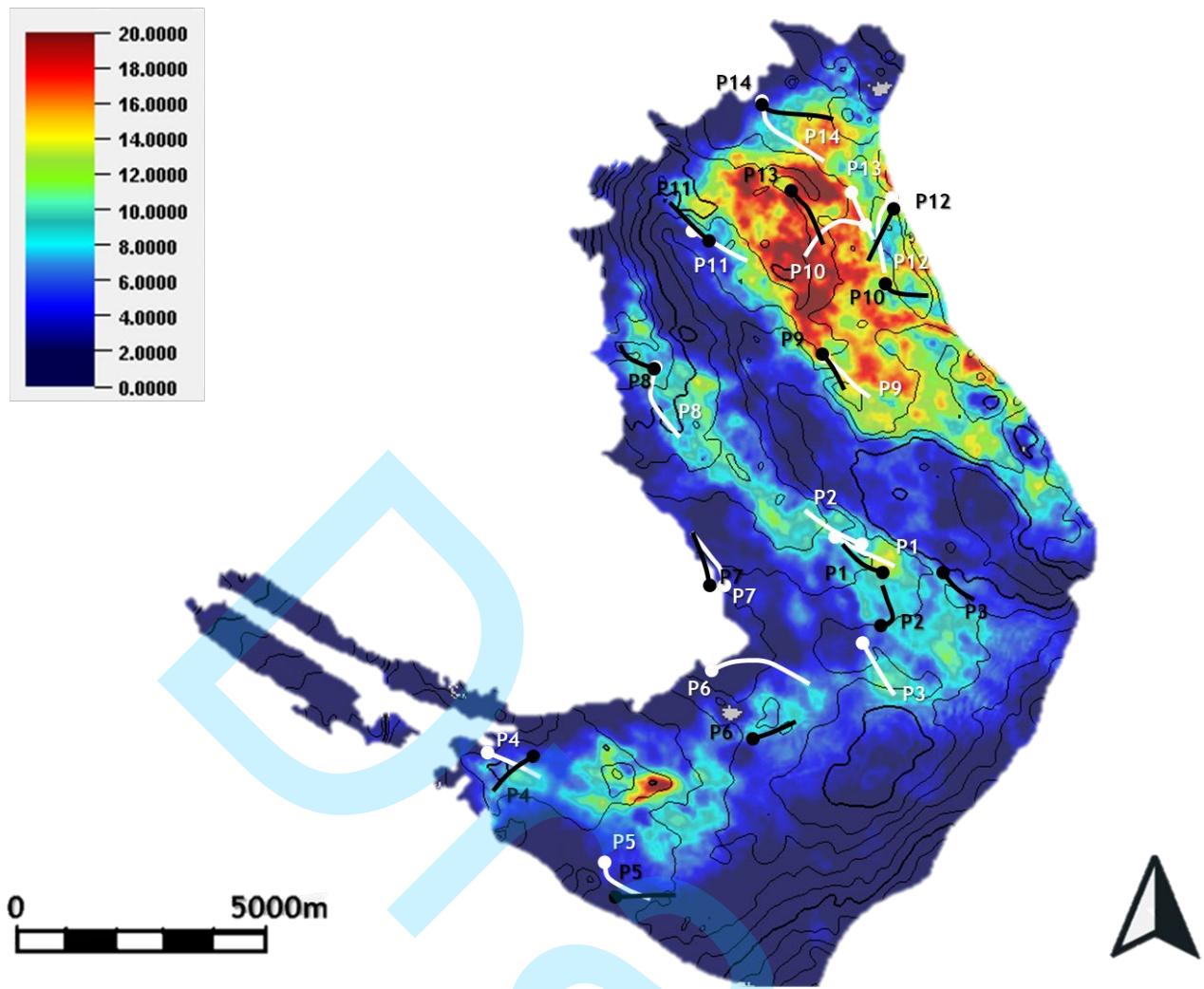
Figure 8 – *Residual oil thickness map estimated from 4D seismic data. It is indicated in the map the location of the original planned producers (in black) and their new locations (in white) after adjusting using 4D seismic data.*

As the Marlim reservoir lacks an active aquifer, the increase in water levels within the reservoir is believed to be solely due to the difference between injected and produced water, which can be observed through production data. On the other hand, 4D seismic data can be utilized to calculate the remaining water volume within the reservoir at each seismic interval. It is possible to perform a quality control (QC) of the results obtained from this approach by comparing the water volume estimated through 4D seismic saturation with the volume determined using production data. The results of this comparison are shown in Table 3.

Table 3 – *Comparison between measured production data and water volume estimated from 4D seismic data.*

Interval	Measured Volume	4D Seismic Volume
2005-1997	242 MM m³	219 MM m³
2010-2005	96 MM m³	114 MM m³
2022-2010	124 MM m³	144 MM m³
Total (2022-1997)	462 MM m³	477 MM m³

From Table 3 it becomes evident that the saturation estimates enabled the retrieval of water volume values that are very similar in terms of orders of magnitude, to those measured. This outcome enhances the reliability of the water saturation estimates.

Another QC measure that was undertaken involved comparing water saturation logs from specific wells with the water saturation level obtained from 4D data. To ensure a thorough and precise analysis, we specifically selected wells that were logged around the same time as the acquisition seismic data. Overall, this QC process revealed a strong correlation between the two datasets, further reinforcing confidence in the methodology employed.

Figure 9 shows some logs for two diferent wells, displaying in the 1st track the gamma ray log, in the 2nd track density an neutron porosity logs, in the 3rd track the resistivity long and in the last track a comparison between water saturation log well data (marked with cyan color) and 4D water saturation estimates (represented by dashed blue lines) extracted along each well from the 4D seismic water saturation variation. Wells 1 and 2 were logged in Aug-2008 and Oct-2012, respectively, and to be as fairy as possible in our comparison, the seismic water saturation log were extracted from the 2010 seismic vintage.   Despite the inherent differences in resolutions between log and seismic data, the 4D water saturation estimates were able to produce values that are reasonably comparable to those observed in the well log data. In the case of Well 1, for example, the water saturation estimates successfully captured an increase in water volume in the middle portion of the reservoir. Similarly, for the Well 2, the 4D water saturation estimates satisfactory identified the rise in water saturation in the lower zone of the reservoir.
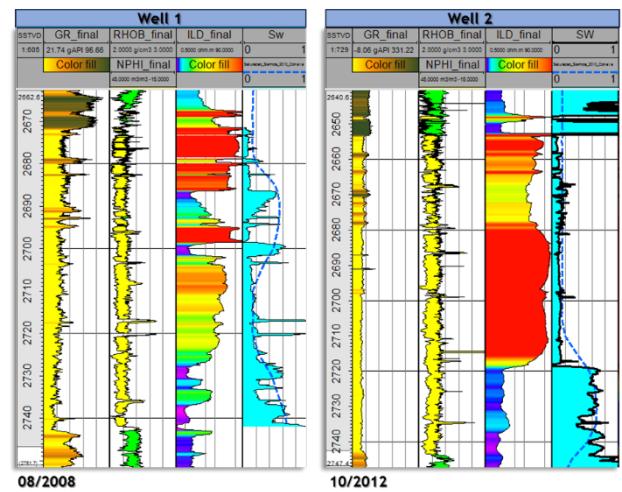

Figure 9 – *Logs from Wells 1 and 2. 1st track shows gamma ray (GR_final); 2nd track: density (RHOB_Final) and neutron porosity (NPHI_Final); 3rd track: resistivity (ILD_Final); 4th track: water saturation (SW); measured in well log (black) and estimated from 4D (dashed blue line).*

In 2021 and 2022, several pre-existing wells were re-logged allowing for the measurement of new values of water saturation along these wells. The water saturation values obtained from these wells, were then compared with the estimates derived from 4D seismic data, as shown in Figure 10. The 6th track, of each well in Figure 10 displays the curves representing the measured residual oil (green) and water saturation (purple), while the dashed blue line represents the estimated water saturation from 4D seismic data. Once again, a strong correspondence between the two datasets can be observed. This quality control (QC) analysis further enhances confidence in the proposed approach and in the reliability of the 4D seismic data itself.

The measured and estimated water saturation values showed in Figure 10 reveal an unexpected increase in water saturation in the upper zone of the reservoir, which is contrary to the anticipated situation where the completion

zone is in the lower zone of the reservoir. This suggests there may have been an error where the injection occurred solely in the upper zone, as seen in the case of the Injector 2, or possibly in both the upper and lower zones, as observed with the Injector 1. This assumption is supported by the temperature log displayed in the 5th track, which indicates injection in these positions, as the injection zone should typically exhibit lower temperatures represented by cold colors.
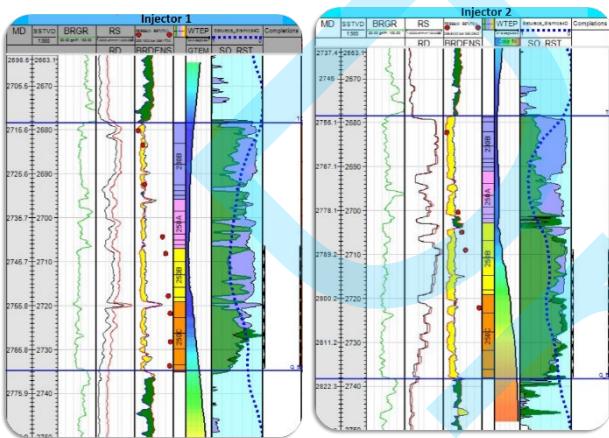

Figure 10 – Well *logs from Injectors 1 and 2. 1st track presents gamma ray (BRGR); 2nd track: shallow resistivity (RS) and deep resistivity (RD); 3rd track: density (BRDENS) and neutron porosity; 4th track: layering; 5th track: temperature (WTEMP); 6th track: oil saturation in green (SO_RST), water moved in purple, original water in cyan and estimated water saturation from 4D in dashed blue line; and 7th track: presents the completion zone.*

Figure 11- A shows the average estimated water saturation map obtained from 4D seismic data covering the period from 2022 to 1997, encompassing the space between the upper and lower reservoir boundaries of the reservoir. Additionally, the map highlights three proposed producer wells (producers 1, 2 and 3) that were identified for REVIT. The presence of the

Injectors 1 and 2 near the proposed producer wells is also indicated on the map. Due to their proximity to the injectors and the fact their initial targets are located in the upper zone of the reservoir (the same zone that the injectors took place) adjustments were necessary for the proposed producer wells.

Furthermore, after making the necessary adjustments to ensure that the well injection zone aligns with the observed depths in the flow model, it was discovered that the oil forecast curves for these proposed wells were significantly affected. As a result, the evaluation of alternative locations become necessary. To identify new suitable positions, the residual oil thickness map was examined. Figure 11-B shows the residual oil thickness map, highlighting the replacement of producers 1 and 2 with new locations.

Indeed, the residual oil thickness map serves as an effective tool for identify areas where significant amounts of oil are still present in the reservoir. However, it is crucial to conduct a comprehensive analysis that combines the 4D dataset with geophysical, geological and engineer data to obtain a robust confirmation of these areas. This multi-disciplinary approach ensures a more accurate understanding of the reservoir and helps in making informed decisions regarding production and development strategies.
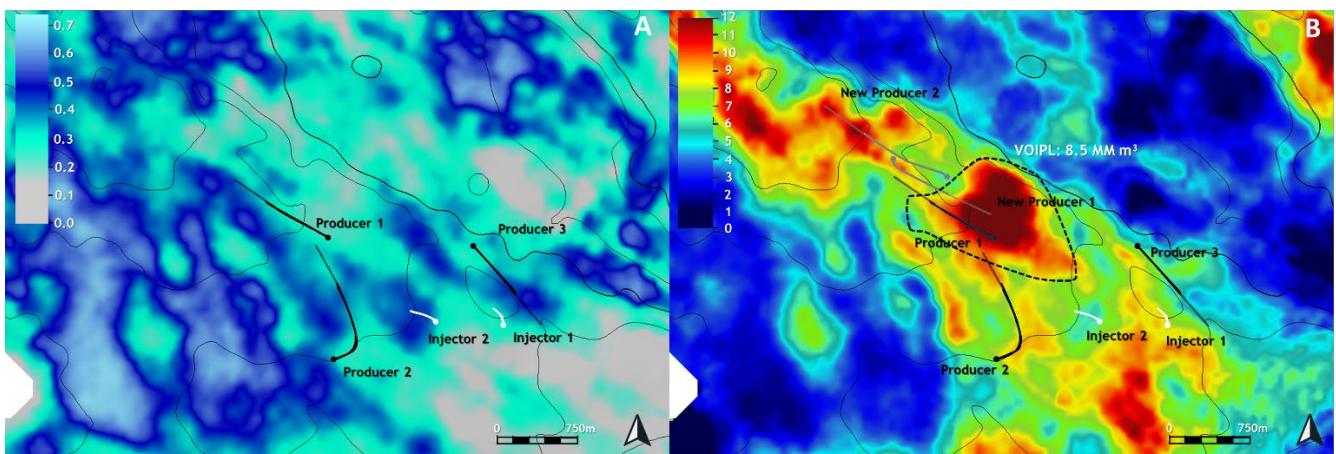
Figure 11 – (A) *Mean estimated water saturation from 4D between 2022 and 1997, highlighting the proposed producers and the existing injectors. (B)* Residual *oil thickness, suggesting unswept areas; a polygon boundary the expected drainage area for New Producer 1 estimated a volume of oil in place of 8.5 MM m³.*

Another advantage of use quantitative attributes is the ability to quantify information. Figure 11-B shows a polygon boundary of the expected drain area for New Producer 1. Within this area, we estimate a volume of oil in place (VOILP) of 8.5 million cubic meters (MM m³). By applying the expected recovery factor of reservoir gain an understanding of how much oil can potentially be produced. This volume can then be compared with the forecasted oil production curve for the respective well, enabling an assessment of reasonableness of the well's oil prediction. This comparison helps in evaluating the feasibility and potential productivity of the well.

In the Marlim reservoir, the drainage strategy typically involves placing injector wells at base reservoir while producer wells are positioned at the top. This strategy may be maintained for New Producer 2 as shown in Figure 11-B. However, for New Producer 1, adjustments were necessary due to its proximity to Injectors 1 and 2. The original drainage strategy could not be maintained in this case, and alternative placement options were explored to optimize production and reservoir management.

Figure 12 shows a 4D water saturation section along New Producer 1. In this figure, a continuous flow of water can be observed along the upper section of the reservoir. The origin of this water flow is connected to Injector 2. What make this figure particularly interesting is that the water not only gets injected into the upper zone of the reservoir but also remains suspended there without descending due to gravity. This suggests the presence of a barrier, like those depicted in Figure 6, that effectively retains the water in the upper zone of the reservoir. In other words, the water is not only injected into the upper zone but also remains there. Based on these observations, it was proposed to position New Producer 1 between the two water levels, as shown in Figure 12.

This location allows for optimal production and management of the reservoir by capturing the oil within the desired zone and minimizing water production.
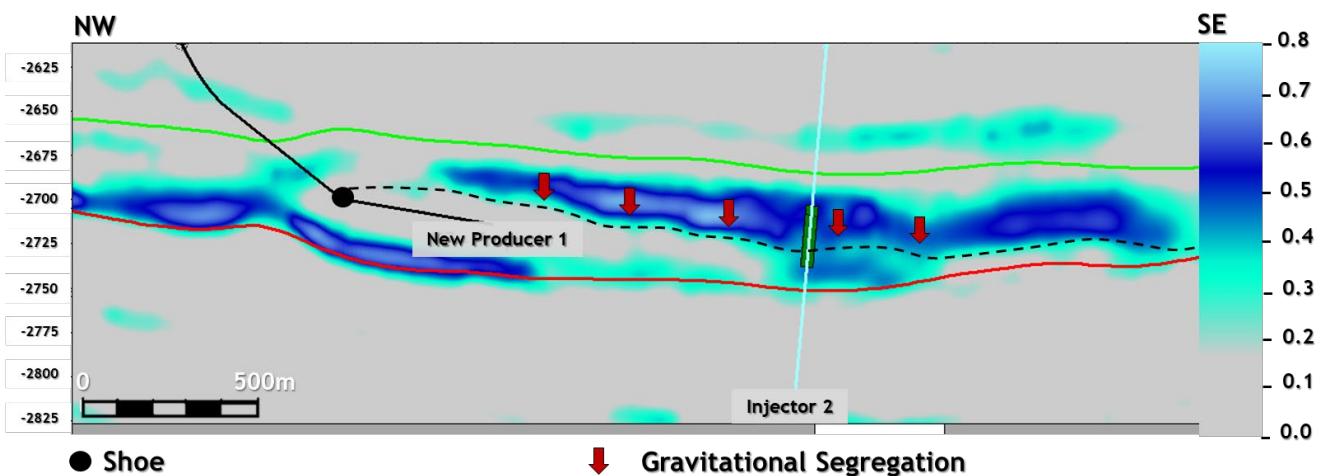
Figure 12 – *Section of 4D water saturation data across New Producer 1. The position of the shoe is indicated in the well and the production section of the well start from this point, with the preceding part isolated to prevent anticipated water production.*

DISCUSSION

As mentioned, the Marlim turbidite reservoir drainage strategy consisted of injecting water at the base and producing oil at the top reservoir. This drainage strategy was highly successful and resulted in very high recovery factor for the reservoir. However, the presence of thin shale barriers has led to detection of water flows at various depths within the reservoir, which has posed a challenge to the drainage strategy in certain areas. Fortunately, the use of 4D data has facilitated the identification of unswept areas and allowed for target adjustments to the drainage strategy. This includes modifying the target of the well, as exemplified by the approach taken for New Producer 1 (Figure 12) and as shown in Figure 13.

In a scenario where water is present at different levels within the reservoir, quantitative attributes such as the residual oil map prove to be more effective than traditional 4D maps. This can be easily observed by comparing Figures 11-A and 11-B.
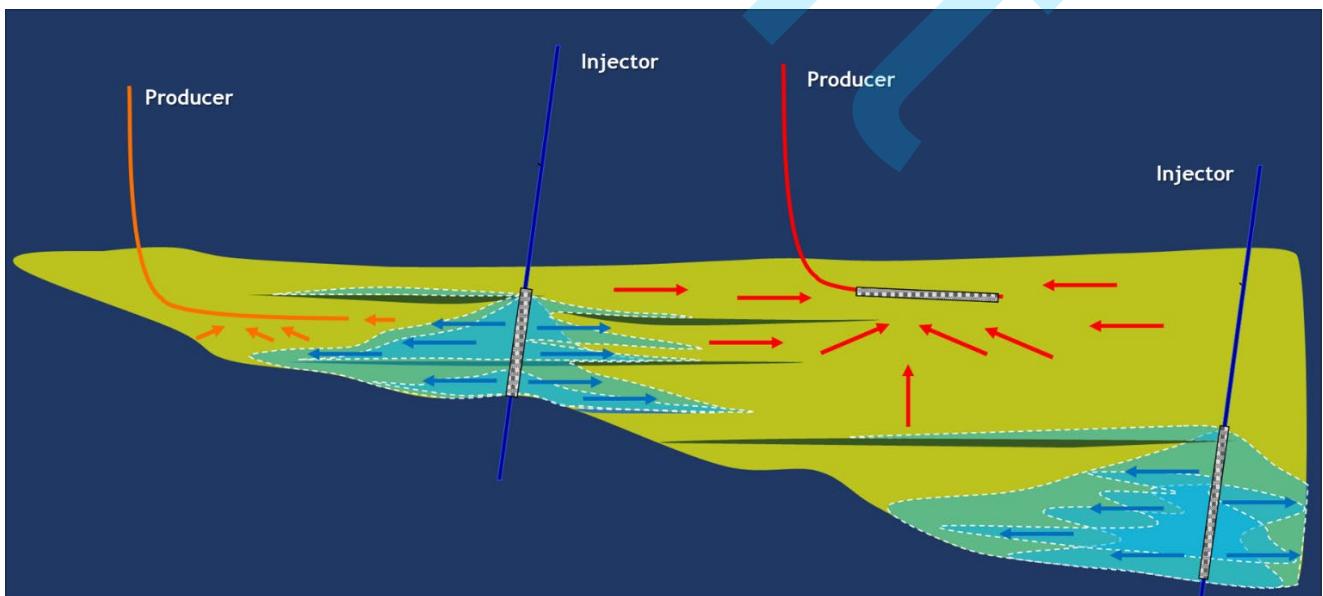
Figure 13 – *Adjusted drainage strategy based on 4D seismic information.*

Regarding the proposed approach, despite its assumptions, quantitative water estimation proved to be an important tool in the Marlim reservoir as it helped identify new opportunities. However, in a more complex reservoir, these assumptions can become very restrictive. In such cases, a thorough understanding of the reservoir can provide valuable insights to apply the approach. For instance, instead of applying the same function for the entire reservoir as we did, defining different functions for different zones can help reduce mismatch and improve accuracy.

Another proposed approach involves the use of scenarios like those shown in Figure 5. In this approach, Case 1 and 2 delineate the boundaries of uncertainties, creating a range of feasible rock physic models between these two curves. By simulating multiple realizations, it becomes possible to choose some among them based on volume criteria, for instance. A more robust approach would involve applying a proper function to each individual voxel, in other words, would be obtaining an inverse function for each voxel based on its properties. This would provide a more accurate and customized analysis for each voxel.

In reservoirs where pressure change occurs, it is crucial to estimate and remove these changes to accurately calculate the saturation, as proposed in this paper. Elastic simultaneous inversions can be utilized to obtain information that allows for the separation of each effect.

CONCLUSIONS

In the Marlim Field, the utilization of 4D seismic technology has significantly improved a better understanding of the reservoir. One key benefit is the identification of preferential paths, which provide valuable anisotropy information and highlight the geological complexity of the reservoir. These paths not only contribute to the construction of more robust reservoir models but also, help identify unswept areas that require further attention. Overall, the insights gained from 4D seismic data play a crucial role in optimizing reservoir management strategies in the Marlim field.

Starting from a simple model composed by the mean properties of the reservoir, we could use Gassmann's equations to calculate the correspondent elastic properties and then establish an inverse function to change P-Impedance variation in water saturation variation. The workflow represents the methodology used to estimate water saturation and, despite its assumptions, has demonstrated consistent results when to observed data such as production measurement and logs. This indicates that, while there may be uncertainties, the baseline scenario applied in the methodology reasonably adheres to the assumptions made for Marlim reservoir. These findings provide confidence in the reliability of the methodology and its ability to accurately estimate water saturation in the reservoir.

The attributes derived from the estimated water saturation, such as residual oil thickness, have proven to be highly valuable tools in identify and delineating potential areas for location adjustments and uncovering new opportunities. However, it is important to emphasize that these attributes, while useful, do not replace the analysis of the original 4D seismic data (amplitude and impedance), 3D seismic data, the conceptual model, well logs, and production data. These additional sources of information

are still critical for a comprehensive understanding of the reservoir and should be considered in conjunction with the derived attributes to make informed decisions.

To summarize, the 4D seismic data and the associated attributes have consistently proven to be important tools for management and understanding throughout the lifetime of the Marlim reservoir. They have played a crucial role in reviewing and optimizing well locations, bringing robustness and speed to the Marlim Revitalization Project. These tools have provided valuable insights and enhanced decision-making processes, ultimately contributing to the efficient and effective management of the reservoir.

ACKNOWLEDGMENTS

REFERENCES

Avseth, P., Mukerji, T. and Mavko, G., 2005. Introduction to rock physics, in Quantitative seismic interpretation. Applying rock physics tools to reduce interpretation risk: Cambridge University Press, UK, Chapter I, 1-47. https://doi.org/10.1017/CBO9780511600074.002.

Batzle, M. and Wang, Z., 1992. Seismic properties of pore fluids. Geophysics, 57, 1396-1408. https://doi.org/10.1190/1.1443207.

Bhakta, T. and Landrø, M., 2014. Estimation of pressure-saturation changes for unconsolidated reservoir rocks with high V_P/V_S ratio. Geophysics 79, M35-M54. https://doi.org/10.1190/geo2013-0434.1.

Boyd-Gorst, J., Fail, P. and Pointing, L., 2001. 4-D time lapse reservoir monitoring of Nelson Field, central North Sea: Successful use of an integrated rock physics model to predict and track reservoir production. The Leading Edge, 20, 1336–1350. https://doi.org/10.1190/1.1487263.

Buland, A. and El Ouair, Y., 2006. Bayesian time-lapse inversion, Geophysics, 71, R43–R48. https://doi.org/10.1190/1.2196874.

Burkhart, T., Hoover, A. R. and Flemings, P. B., 2000. Time-lapse (4-D) seismic monitoring of primary production of turbidite reservoirs at South Timbalier Block 295, offshore Louisiana, Gulf of Mexico. Geophysics, 65, 351–367, https://doi.org/10.1190/1.1444731.

Cruz, N. M., Cruz, J. M., Teixeira, L. M., Costa, M. M., Oliveira, L. B., Urasaki, E. N., Bispo, T. P., Jardim, M. S., Grochau, M. H. and Maul, A, 2021. Tupi Nodes pilot: A successful 4D seismic case for Brazilian presalt reservoirs. The Leading Edge, 40, 866-896. https://doi.org/10.1190/tle40120886.1.

Damasceno, A., 2020. 4D Quantitative Interpretation of Jubarte Field (Brazil): An Integrated Approach. Master's degree dissertation, Colorado School of Mines.

Damasceno, A., Tura, A., Vasquez, G., Ramos, W. and Dariva, P., 2021. Integrating rock physics, PP-PS joint inversion and time-shifts to improve quantitative interpretation of time-lapse fluid and pressure changes. First Break, 39, 53-60. https://doi.org/10.3997/1365-2397.fb2021068.

Floricich, M., MacBeth, C. and Staples, R., 2005. An engineering-driven approach for separating pressure and saturation using 4D seismic. Application to a Jurassic reservoir in the UK North Sea. 75th SEG Meeting, Houston, USA, Expanded Abstracts.

Gassmann, F., 1951 Uber die elastizität poröser medien. Vierteljahrsschr. Naturf. Ges. Zürich., 96, 1- 23.

Grochau, M. and Gurevich, B., 2008. Testing Gassmann fluid substitution: sonic logs versus ultrasonic core measurements. Geophysical Prospecting, 57, 75-79. https://doi.org/10.1111/j.1365-2478.2008.00726.x.

Grochau, M., Benac, P., Alvim, L., Sansonowski, R., Pires, P. and Villaudy, F., 2014. Brazilian carbonate reservoir: A successful seismic time-lapse monitoring study. The Leading Edge, 33. https://doi.org/10.1190/tle33020164.1.

Johann, P., Thedy, E., Gomes, F. and Schinelli, M, 2006. 4D seismic in Brazil: Experiences in reservoir monitoring. Presented at the Offshore Technology Conference. https://doi.org/10.4043/18400-MS.

Johnston, D.H., 2013. Practical Applications of Time-Lapse Seismic Data. SEG Distinguished Instructor Series, No. 16, Society of Exploration Geophysicists. 289pp. https://doi.org/10.1190/1.9781560803126.

Lafet, Y., Roure, B., Doyen, P. M., Bornard, R., Buran, H. and Smith, A., 2008. Global 4-D seismic inversion and time-lapse fluid prediction, 70th EAGE Conference Expanded Abstracts, pp. 5. DOI: 10.1190/sbgf2009-405.

Landrø, M., 2001. Discrimination between pressure and fluid saturation changes from time-lapse seismic data. Geophysics 66, 836–844. https://doi.org/10.1190/1.1444973.

Landrø, M., Solheim, O. A., Hilde, E., Ekren, B. O. and Strønen, L. K., 1999. The Gullfaks 4D seismic study. Petroleum Geoscience, 5, 213-226. https://doi.org/10.1144/petgeo.5.3.213.

Landrø, M., Veire, H. H., Duffaut, K. and Najjar, N., 2003. Discrimination between pressure and fluid saturation changes from marine multicomponent time-lapse seismic data. Geophysics, 68, 1592–1599. https://doi.org/10.1190/1.1620633.

Lumley, D., Meadows, M., Cole, S. and Adams, D., 2003. Estimation of reservoir pressure and saturations by crossplot inversion of 4D seismic attributes, 1513–1516. SEG Technical Program Expanded Abstracts 2003. Society of Exploration Geophysicists. https://doi.org/10.1190/1.1817582.

MacBeth, C., Floricich, M. and Soldo, J., 2006. Going quantitative with 4D seismic analysis. Geophysical Prospecting, 54, 303-317. https://doi.org/10.1111/j.1365-2478.2006.00536.x.

Oliveira, R. M., Bampi, D., Sansonowski, R. C., Ribeiro, N. M. S., Johann, P. R. S., Santos, M. S. and Ferreira, D. M., 2007. Marlim Field: Incorporating 4D Seismic in the Geological Model and Application in Reservoir Management Decisions. Latin American & Caribbean Petroleum Engineering Conference, Buenos Aires, Argentina, April 2007.

Rasolofosaon, P. N. and Zinszner, B. E., 2007. The unreasonable success of Gassmann's theory… Revisited. Journal of Seismic Exploration, 16(2), 281-301.

Ribeiro C., and MacBeth C., 2004. A petroelastic-based approach to pressure and saturation estimation using 4D seismic. 66th SEG Technical Program Expanded Abstracts, 2271-2274. https://doi.org/10.1190/1.1845215.

Ribeiro, N. M., Steagall, D., Oliveira, R., Formiga, L., Kerber, P. and Jarger, M., 2005. Challenges of the 4D seismic in the reservoir management of the Marlim Field: SPE94905 Latin American & Caribbean Petroleum Engineering Conference, Rio de Janeiro, Brazil, June 2005. https://doi.org/10.2118/94905-MS.

Rosa, D. R., Santos, J. M. C., Souza, R. M., Grana, D. and Schiozer, D. J., 2020. Comparing different approaches of time-lapse seismic inversion. Journal of Geophysics and Engineering, 17, 929-939, Oxford. https://doi.org/10.1093/jge/gxaa053.

Sansonowski, R. C., Oliveira, R. M., Ribeiro, N. M., Bampi, D. and Camarão, L. F., 2007. 4D Seismic interpretation in the Marlim Field, Campos Basin, offshore Brazil: 10th International Congress of the Brazilian Geophysical Society, Rio de Janeiro, Brazil. https://doi.org/10.1190/sbgf2007-479.

Sarkar, S., Gouveia, W. P. and Johnston, D. H., 2003. On the inversion of time-lapse seismic data, SEG Technical Program Expanded Abstracts, 1489–1492. https://doi.org/10.1190/1.1817575.

Smith, T. D., Sondergeld, C. H. and Rai, C. S., 2003: Gassmann fluid substitutions: A tutorial. Geophysics, 68, 430-440. https://doi.org/10.1190/1.1567211.

Veeken, P. C. H. and Da Silva, M., 2004. Seismic Inversion Methods and some of their constraints: First Break, 22, 47-70. https://doi.org/10.3997/1365-2397.2004011.

Villaudy, F., Lucet, N., Grochau, M. and Benac, P., 2013. 4D simultaneous pre-stack inversion in an offshore carbonate reservoir. Conference: 13th International Congress of the Brazilian Geophysical Society & EXPOGEF, Rio de Janeiro, Brazil. DOI:10.1190/sbgf2013-211.

Webb, B., Salerno, S., Rizzetto, C., Panizzardi, J., Marchesini, M., Fervari, M., De Draganich, C., Colombi, N. and Calderoni, M., 2020. A time-lapse case study in West Africa: Integrating disciplines for a complete reservoir study and field management. The Leading Edge, 39, 110–118. https://doi.org/10.1190/tle39020110.1.

Matto Grosso da Silva, C.J.: Elaborated the approach and applied it on Marlim reservoir and evaluated, by perform quality control, its results. Discuss and interpret the 4D results and proposed adjustments for the new wells based on 4D data and the approach results. Wrote and review this manuscript; **Benac, P.:** Elaborated the approach and review this manuscript; **Botelho, E.S.:** Participating in the discussion of 4D results and adjusts of well locations; **Giro, H.M.:** Participating in the discussion of 4D results and adjusts of well locations; **Lima, R.:** Participating in the discussion of 4D results and adjusts of well locations; **Santos, P.F.:** Participating in the discussion of 4D results and adjusts of well locations; **Garcia, M.D.A.:** Participating in the discussion of 4D results and adjusts of well locations; **Da Costa, T. C.:** Participating in the discussion of 4D results and adjusts of well locations; **Pedrosa, C.A.:** Participating in the discussion of 4D results and adjusts of well locations.